A brightening coronal loop observed by TRACE: II. Loop modeling and constraints on heating.

F. Reale, G. Peres, S. Serio[a], R. M. Betta[1]

Dip. di Scienze Fisiche & Astronomiche – Sez. di Astronomia – Univ. di Palermo, Piazza del Parlamento 1, I–90134 Palermo, Italy

[a]*Osservatorio Astronomico, Piazza del Parlamento 1, I–90134, Palermo, Italy*

E. E. DeLuca, L. Golub

Smithsonian Astrophysical Observatory, 60 Garden Street, Cambridge, MA 02138, USA

ABSTRACT

This is the second of two papers dedicated to the brightening of a coronal loop observed by TRACE on 26 June 1998; it aims at hydrodynamic modeling the brightening. Since the loop geometry is practically unchanged during the brightening, the evolution of the plasma confined in the loop is described with a one-dimensional hydrodynamic time-dependent numerical model and from the results the emission along the loop in the TRACE 171 Å band is synthesized. The information from Paper I is used to derive the geometry and the initial configuration of the loop, as well as for comparison with the results of the model. The modeling is focused to determine the amount, spatial distribution and evolution of the heating deposited in the loop to make the modelled evolution close to that observed with TRACE. We find that, in order to match the observed evolution and distribution of the brightness along the loop, the heating has to be non-symmetrical in the loop, in particular deposited between the apex and one footpoint (3×10^9 cm from the southern footpoint). A reasonable match with observations is obtained by assuming that the heating is switched on abruptly and then kept constant for the whole rising phase. An even better match is obtained with the heating high and constant for 100 s and then decaying exponentially with an e-folding time of 300 s. We discuss the resulting physical scenario: a bright irregular structure close to the loop in the TRACE images may be a tracer of the heating release.

Subject headings: Sun: activity, Sun: corona

[1]Now at Dipartimento di Fisica, Università di Pisa, Piazza Torricelli, 2 56126 Pisa, Italy

1. Introduction

This study is devoted to the interpretation and modeling of the evolution of the brightening of a coronal loop observed with the Transition Region And Coronal Explorer (TRACE) at an unprecedented level of spatial detail and temporal cadence. In Paper I (Reale et al. 1999) we have analyzed the data, described in detail the loop morphology and evolution, and derived the main physical characteristics of the emitting plasma. This paper is devoted to the detailed physical modeling of part of the event and to the diagnostic of the heating process which ignites the loop. As shown in Paper I, the loop geometry remains unchanged during the observation, even though the emission is variable and highly transient. This allows us to assume that the emitting plasma is always confined inside the loop and moves only along the magnetic field lines. We can therefore model the plasma evolution by means of a one-dimensional time-dependent hydrodynamic model.

Since the loop geometry is well defined and does not change, one can assume that the role of the magnetic field is limited to confining the plasma, with no strong effect on the plasma dynamics; this leaves a relatively small set of free parameters, and the modeling becomes a powerful tool to gain insight into the plasma physical evolution and to constrain the heating process, in particular its location and timing.

Loop plasma modeling has been well established since the solar coronal structuring has been identified (e.g. Vaiana et al. 1973). Hydrostatic loop models have been used extensively since the pioneering effort of Rosner et al. (1978), Vesecky et al. (1979), Serio et al. (1981). Other steady-state loop models consider steady siphon flows driven by a pressure difference between the footpoints (Cargill & Priest 1980, Noci 1981, Mariska & Boris 1983, Antiochos 1984, Orlando et al. 1995). As for time-dependent models, hydrodynamic numerical approaches have been extensively used to model solar flaring loops (e.g. Nagai 1980, Peres et al. 1982, Doscheck et al. 1983, Nagai & Emslie 1984, Fisher et al. 1985, MacNeice 1986, Gan et al. 1991, Reale & Peres 1995, Hori et al. 1997). Some modeling of the evolution of non-flaring loops, analogous to that presented here, has addressed the general problem of coronal heating, and in particular heating by microflares (e.g. Peres et al. 1993, Kopp and Poletto 1993).

Our approach here is to use hydrodynamic modeling to simulate in detail the temporal evolution of the plasma distributed along a specific loop observed by TRACE (Paper I) and to synthesize its emission as detected in the focal plane of TRACE. This allows us to make direct comparison with the observation, to draw a feedback on the model and to obtain diagnostic information. Although we will not attempt a detailed formal fit to the data, by matching a series of observational constraints we will try to answer the questions listed at the end of Paper I, i.e. what heats and turns the loop on? How is the heating related to changes in adjacent structures? How does the heating evolve?

In section 2 we outline the observational constraints that we attempt to match. The modeling is described in section 3, results are reported in section 4 and discussed in section 5.

2. A summary of the observational constraints

Fig.1 shows a sketch of loop L_4, object of this study, and of the main structures surrounding it. At the beginning of the observation it is not visible, but very dynamic events occur in the surrounding region: a luminous blob appears to travel along a magnetic flux tube (L_2) and bifurcates traveling along two separate and diverging loops (L_2 and L_3). Afterwards a bright and filamentary knot (structure B), with a linear size of $\sim$ 15", remains bright throughout the rest of the observation ($\sim$ 2 hours), although highly filamented and variable, at the bifurcation of L_2 and L_3. As we will discuss in Section 5, the hydrodynamic modeling and the inferred timing and location of the heating suggest that these preliminary events may be fundamentally tied to the brightening of L_4 which occurs afterwards.

Well after the blob has completed its travel, the loop of interest becomes gradually visible, starting from the footpoints, half an hour after the beginning of the observation. Moving bright fronts rise coherently from the footpoints, first from the northern one ($t \sim 2500$ s) and then from the southern one ($t \sim 2900$ s). This behavior may suggest the propagation of temperature and/or density fronts from the footpoints to the apex. The whole loop then becomes clearly visible; it appears to be slanted with respect to the surface, probably at an angle of $\approx 60°$ from the vertical, and with a total length $\approx 1.0 \times 10^{10}$ cm. At its maximum luminosity, the brightness distribution appears asymmetric along the loop, the northern footpoint being brighter than the southern one. The footpoints are, for most of the time, brighter than the apex by a factor ≥ 3.

As discussed in Sect. 3.2 our choice has been to model a semicircular arch with the same length as the observed loop. The difference of the observed loop from a semicircular one is not relevant for our modeling. Figure 2 shows the background subtracted brightness distributions along the loop L_4 observed by TRACE in the 171 Å band during the rising phase of the brightening[2]. The loop-shaped images are obtained by averaging the brightness in sectors 4 pixels wide and 10 pixels long (2×5 arcsec) along the loop (as illustrated in Paper I) and then mapping the average values into one-dimensional semicircular arches. The left footpoint corresponds to the southern footpoint in the observation. This format makes the data more easily comparable to the modeling results. Loop filamentation is not very evident during the rising phase, when filaments appear to evolve coherently. The averaging process therefore degrades virtually no information important for our modeling. After the rising phase the filaments no longer evolve coherently and follow slightly different evolutions. The study of the late evolution of the loop is postponed to a future work. We focus the present modeling on the rising phase in the light of the coherent evolution of the brightness across the loop.

From Fig.2 we see that before t=2239 sec only faint loop legs are visible in the chosen brightness scale, and a faint blob in the southern leg, which is the signature of structure B. Therefore it does not belong to the loop, and is only aligned with it. At t=2359 sec the arch is almost all visible. At t=2717 sec the northern (right) leg is much brighter than the other and than before: a bright front is coming up from the footpoint. At t=2956 sec the other leg also becomes bright, as an effect of another bright front from the southern footpoint. After the two fronts join, at $t \sim 3100$ sec, the loop is wholly bright, but the brightness distribution is distinctly asymmetric, the right leg remaining brighter than the other leg.

In Paper I we have estimated that the confined plasma has a density $\sim 6 \times 10^8$ cm^{-3} close to the loop apex and at the maximum of the loop luminosity, corresponding to a pressure of the order of 0.1 dyne cm^{-2}, if we assume a temperature of 1 MK, namely the temperature of maximum formation of FeIX, the ion making the predominant line in the TRACE 171 Å band. The e-folding rise time of the loop light curve is ~ 800 s while the decay time is much longer, i.e. > 6000 s.

[2]An animation of the sequence is available at http://www.astropa.unipa.it/....

3. The model

3.1. The approach

We work under the hypotheses that: a) initially the plasma in the loop is not at coronal temperatures ($T \ll 10^6$ K) and the loop is almost empty, since it is totally invisible to TRACE at the beginning of the observation; b) its brightening is caused by the transient release of heating somewhere inside it, which leads the plasma temperature in the range of TRACE sensitivity, and increases the emission measure by driving evaporation of plasma from the chromosphere.

We exclude that what we see is due to the simple cooling of a hot loop for the following reason: such a hot loop (say 3-5 MK) if initially close to a steady state condition, would also be filled by rather dense plasma according to the loop scaling laws. The loop emission measure would therefore be very high since the beginning. We have checked (Reale & Peres 1999) that, even if at those high temperatures the 171 A filter response is reduced by more than two orders of magnitude from its maximum, still it is well above zero and the high emission measure would make the loop well visible by TRACE, with respect to other cooler structures along the same line of sight. In conclusion the whole hot loop would be well visible by TRACE already since the beginning of the observation, contrary to observations. One may then think that the loop is initially hot but still far from equilibrium, i.e. not filled up with dense plasma. This implies a heating active for a short time and then switched off more or less gradually: but, as we will see (section 4.2.2), this is exactly our model which best reproduces the observed evolution and brightness distributions.

The loop is assumed to be a closed flux tube where plasma motion and heat flux are parallel to the field lines. The plasma is described as a single compressible fluid by solving numerically the time-dependent one-dimensional hydrodynamic equations of mass, momentum and energy conservation, together with the appropriate equation of state, as in Peres et al. (1982). The effects of the gravity component along the loop, of compressional viscosity, of hydrogen ionization potential, of classical plasma thermal conduction (Spitzer 1962), of radiative losses from an optically thin plasma (Raymond & Smith 1977) with standard solar photospheric abundances are included (Rosner et al. 1978). Using different abundances, such as those suggested by Feldmann (1992), would have little or no effect on the initial loop plasma evolution, which we address here, and which is governed by dynamics and thermal conduction. A time-dependent function Q accounts for the heating source necessary to bring the plasma to coronal conditions. The coronal solutions are matched with one of the chromospheric models of Vernazza, Avrett and Loeser (1981) for temperatures $T \leq 2 \times 10^4$ K. The base of the loop is fixed in the chromosphere at the minimum temperature $T = 4400$ K.

An appropriate spatial numerical resolution is granted everywhere along the loop by means of appropriate spacing and regridding algorithms (Betta et al. 1997). We use a recent version of the code which allows for the description of evolution in a non-symmetrical loop (Betta 1998). Previous versions solved the equation along half of the loop, assuming symmetry with respect to the loop apex. The new approach is fundamental since we need to explain the asymmetric distribution of the brightness along the loop and its asymmetric evolution.

The heating $Q(s,t)$ is assumed to be a separable function of space and time, as in previous works (e.g. Peres et al. 1987):

$$Q(s,t) = H_0 \; f(t) \; g(s) \tag{1}$$

where s is the coordinate along the loop, t is the time. We consider a gaussian spatial distribution:

$$g(s) = \exp\left[-\frac{(s-s_0)^2}{2\sigma^2}\right] \tag{2}$$

where s_0 is the central coordinate of the region along the loop where the heating is released, σ is the half-width of the gaussian. This functional form describes a heating at a fixed location along the loop. Although our numerical model includes the option for heating by non-thermal electron beams, we did not explore this possibility in detail for the reason discussed in Sect. 5.

As for the time dependence $f(t)$, we will consider the following functional form:

$$f(t) = \begin{cases} 1 & 0 \leq t \leq t_0 \\ \exp\left(\frac{t_0 - t}{\tau}\right) & t > t_0 \end{cases} \tag{3}$$

and, in particular, either a heating abruptly switched on, maintained constant for a given time lapse and then switched off immediately ($\tau = 0$, Sect. 4.1), or a heating high for a short time interval, and then exponentially decaying ($\tau > 0$, Sect. 4.2).

The evolution of plasma density, temperature and velocity is computed over a time interval of a few thousands seconds, comparable to the duration of the observed loop rising phase. From these quantities we synthesize the emission per unit volume along the loop in the TRACE 171 Å band as:

$$\mathcal{E}(s,t) = n^2(s,t) \; G[T(s,t)] \tag{4}$$

where n is the plasma density, $G(T)$ the plasma emissivity at temperature T per unit emission measure and solid angle folded with the instrument spectral response in the 171 Å filter band. $G(T)$ has been computed by using the MEKAL spectral code (Mewe et al. 1995), assuming standard solar abundances. Enhanced abundances (e.g. Feldmann 1992) would determine a self-similar increase of G(T), would change the absolute emission value, but not the evolution and the shape of the brightness distribution along the loop, which depend mainly on the shape of the response profile vs temperature. Equation (4) is used to derive the brightness distributions along the loop which can be compared to the re-mapped observed ones. In order to derive from the models the flux measured by TRACE, a conversion factor α from emission per unit volume to flux $\mathcal{F}$ at the instrument focal plane is needed. This conversion factor has the units of a length and is derived as:

$$\mathcal{F} \approx \mathcal{E}\frac{V}{A} \approx d_l \mathcal{E} \tag{5}$$

where V is the plasma volume inside a pixel along the line of sight, A is the pixel area and $d_l = \alpha$ is the plasma thickness along the line of sight. Our ignorance of the loop plasma filling factor, associated with the filamentation, causes uncertainties on the evaluation of α. We estimate $\alpha \sim 10^9$ cm, of the same order as the estimated loop thickness (cf. Paper I). Finally, we need to derive a lower limit for signal detectable above background level in order to discriminate detectable from undetectable effects. We will take a background value itself as a reasonable lower limit. From an inspection of the background subtracted brightness profiles (Fig.6 in Paper I), a reasonable background level is $\mathcal{F}_{min} \sim 0.1$ DN/s/pix, which corresponds to $\mathcal{E}_{min} \sim 10^{-10}$ DN cm^{-3} s^{-1} pix^{-1}.

3.2. The modeled loop

The loop geometry, and in particular its orientation with respect to the vertical direction, has been thoroughly discussed in Paper I. The conclusion has been that the loop can be reasonably assumed to be inclined by 60° with respect to the vertical to the surface.

For the sake of completeness, and as a further check, we have performed hydrodynamic simulations of a loop both perpendicular and tangent to the solar surface. As discussed in Paper I, the real length of a perpendicular loop would be much larger than the measured (projected) one and it would be so elongated to be rather difficult to explain. We assume a loop 3×10^{10} cm long, initially empty and invisible to TRACE, and a heating rate adequate to make the loop reach approximately a temperature in the TRACE sensitivity range. The heating makes chromospheric plasma expand upwards, and therefore the plasma density (and the emission) increase from the footpoints toward the apex. However, since the loop is very long and extends well above the pressure scale height (which is $sim 5 \times 10^9$ cm at 1 MK), the density in the upper section of the loop would be much lower than at the footpoints at any time, and the loop apex would be totally invisible to TRACE at any time, contrary to what is observed. The same occurs if we increase the heating rate to evaporate more material, because the temperature at the apex would increase out of the range of TRACE sensitivity. We conclude that a vertical loop can hardly agree with the observation and that an inclined loop is a more reasonable assumption.

As for the loop tangent to the solar surface, a related simulation has been done for a loop 10^{10} cm long, a maximum gravity component $g = 0.1\ g_{\odot}$, and an initial temperature of 2×10^4 K. Even at such a low temperature, the loop apex is below the pressure scale height. The loop is then full of plasma, and the heating produces only a weak chromospheric evaporation and a gradual increase of the temperature along the loop. The result is that TRACE would see only some segments of the loop at a time, far from the footpoints and changing with time and the loop footpoints would be invisible at the beginning. This is totally in contrast with the observation and makes us exclude that the loop is tangent to the surface.

We assume a loop inclined by 60° and a total loop length[3] $L = 10^{10}$ cm. We also assume that the plasma is, at initial time, isothermal at $T = 5 \times 10^4$ K, with a pressure of 0.01 dyne cm^{-2} at the footpoints. The loop extends to a height $\sim 1.5 \times 10^9$ cm above the surface. Since the pressure scale height for such a plasma is $\approx 2.5 \times 10^8$ cm, initially the loop is practically empty. Assuming that the loop is semicircular, while it is, most likely, slightly elongated, is inconsequential at all times of the simulations. The only effect of the elongation is, in fact, to change the gravity component along the loop, and gravity has essentially no importance in the initial impulsive evolution of the loop; its role is confined to determine the stratification of the initial atmosphere and this is in turn ineffective as long as the initial loop is constrained to be practically empty. Fig. 3 shows a sketch of the assumed loop geometry and of the three locations of the heating that we shall discuss in the following.

The preliminary simulations discussed above show that the loop geometry and initial conditions cannot be very different from the ones just listed, i.e. an inclined, initially empty and cool loop. The fact that we are able to constrain them is, on the one hand, an interesting result by itself, and on the other it makes our study self-consistent and reduces the number of free parameters in our further steps.

4. The model results

4.1. Constant heating

We now study the evolution of the model loop when subject to a transient heating. Our basic questions are now: what is the intensity of the heating, where is it released, and, possibly, what is its evolution?

A fundamental aspect to answer the first question is that the heating rate should be enough to bring the loop to a temperature around 1 MK. Due to its thermal conductivity the plasma is heated to a steady-state temperature very rapidly. A good estimate of the heating rate for a loop at 1 MK can be provided by the scaling laws derived for hydrostatic coronal loops (Rosner et al. 1978), even when the loop is not exactly in hydrostatic equilibrium.

The second question, the location of the heat release, is instead much less trivial to answer, and it is one of the crucial questions investigated in this work. Our approach to solve this problem is to make a few

[3] Correcting for projection yields a length of $\approx 1.1 \times 10^{10}$ cm.

educated guesses, to compute the relevant evolution of the confined plasma and of its brightness, and to examine which of the alternative cases best matches the observed loop brightness evolution.

We will turn to the third question, the evolution of the heating, later in this work (Sect.4.2). For the moment we will assume that the heating is suddenly switched on at its maximum intensity and then kept constant for the whole duration of the simulations (3000 sec). This will allow us to focus first on the question of the location of heat release.

In order to constrain the location, we model the plasma loop evolution for different values of s_0 and σ (see Fig. 3), and compare the results with observations. We distinguish five main cases: A) heating released at one footpoint; B) heating released uniformly along the loop; C) heating released asymmetrically between the apex and one footpoint; D) heating at the loop apex; E) heating released at both footpoints. We will not discuss the case D) because, as shown by the case of uniform heating B), any kind of symmetric heating can be excluded. Case E) will not be computed and it can be excluded for the reasons presented in Section 5. The parameters of the simulations are shown in Table 4.1.

4.1.1. Heating at one footpoint

The observation shows us that the northern footpoint is always brighter than the southern one, and that earlier and more intense brightness fronts move from it. This may suggest that the northern footpoint is the site of the heating. This hypothesis is explored with model A in Table 4.1.

At t = 0 s the heating is switched on at the left (in the model) footpoint. Fig. 4 shows the evolution of the plasma temperature, density, pressure and velocity along the loop, as well as the emission in the TRACE 171 Å synthesized according to Equation (4). In the last panel, the data are also shown for reference; however, any comparison of model results to data in this figure, as well as in Figs.6, 7, 8, should be taken with care because the data are binned over sections of several pixels along the loop and because the lower limit of the measured brightness profile (see the lower data profile) is dictated by the background noise and not only by the intrinsic loop brightness, which may be much lower than the measured value.

As shown in the upper left panel of Fig.4, the temperature increases rapidly at the left footpoint, reaching $\sim 7 \times 10^5$ K in less than one minute. A conduction front propagates from the left footpoint, and reaches the other footpoint after ~ 10 minutes. The conduction front slightly precedes an "evaporation" front of dense plasma arising from the chromosphere at the left footpoint, with a maximum speed increasing in time from 100 to 200 km/s. When the evaporation front arrives at the right footpoint, the plasma is compressed there and a second strong pressure front develops and moves backward to the left footpoint, reaching it after approximately other 1000 seconds ($t \approx 1500$ s). This second pressure front is an accumulation front, since the plasma velocity is rightward (positive) at any time. For $t > 1500$ sec, the plasma settles to a much less dynamic state: the temperature is almost uniform at ≈ 1 MK, the density increases almost uniformly to $\sim 5 \times 10^8$ cm^{-3}, and the velocity is reduced to less than 50 km/s.

The evolution of the plasma brightness is roughly similar to that of the density, but the moving fronts are much steeper. For an easier comparison to the observed evolution (see Fig. 2), Fig. 5 shows distributions of the brightness along the model loop at various times as grey-scale loop images[4]. Summarizing results of model A, in the TRACE band, a first, relatively weak (barely detectable) brightness front moves from the left footpoint, and fades away when it approaches the right footpoint. Then a second much brighter front propagates leftwards from the right footpoint. During this phase the right footpoint is much brighter than the left one. The loop becomes wholly visible after ~ 1300 sec, with the right leg being brighter than the left one at this time. The brightness then becomes progressively more uniform, although the right footpoint, opposite to that where the heating is deposited, remains the brighter one.

This evolution of the brightness along the loop is highly asymmetric: first the heated footpoint brightens, although at a low level; then, much later, the opposite footpoint brightens; it becomes much brighter than the former; the heated leg is fainter than the not heated one. This evolution is *not* in agreement with the observed one, which shows that the loop legs brighten almost synchronously and certainly not in alternation. Only the final (t= 3000 s in Fig.4) brightness distribution resembles quite closely the brightness distribution observed near the time of maximum

[4]An animation of the sequence is available at http://www.astropa.unipa.it/....

Table 1: Parameters of the simulations with transient constant heating

Name	Location	H_0 (10^{-3} erg cm^{-3} s^{-1})	s_0 (10^9 cm)	σ (10^9 cm)	t_0 (sec)	τ (sec)
A	Footpoint	10	0.3	0.05	3000	0
B	Uniform	0.07	–	–	3000	0
C	Asymmetric	0.4	3	0.5	3000	0
C'	Asymmetric	4	3	0.5	100	300

loop luminosity. According to the results of model A, we conclude that *it is unlikely that the heating is deposited at one footpoint*. It is worth noting that for most of the time the brighter leg is the opposite to the heated one. This leads us to think that the heating is likely deposited in the *southern* leg, and, once again, confirms that the heating location is not trivially connected to the regions where the coronal loops are bright in the XUV band (e.g. Reale & Peres 1995).

4.1.2. Uniform heating

Although the moderate asymmetry of the observed evolution requires some level of asymmetry of the heat source with respect to the loop axis, we have also explored the case of an almost uniformly heated loop, i.e. the opposite extreme of the one footpoint heating. This will help us both to have a complete scenario of the possible plasma physical evolution and to evaluate how significant are the observed deviations from a symmetric evolution.

Fig.6 shows the plasma evolution of the model loop heated uniformly (Model B in Table 4.1). Of course the plasma evolution is entirely symmetric with respect to the loop apex. The temperature increases anywhere in the loop almost at the same rate, slightly more rapidly at the apex, where the density, and therefore the heat capacity, is smaller. After ~ 100 s almost the entire loop is at a temperature of ~ 1 MK. The overpressure which develops at the footpoints makes dense plasma evaporate from the chromosphere. The twin evaporation fronts toward the loop apex are more gentle than the fronts in the footpoint-heated model, as shown by the velocity profiles (≤ 100 km/s). The final density and temperature distributions are obviously fully symmetric with respect to the apex: the temperature has a maximum and the density has a minimum exactly at the loop apex. The temperature at the loop apex settles to a value around 1.5 MK and the density at $\sim 3 \times 10^8$ cm^{-3}.

The last panel of Fig. 6 shows the symmetric evolution of the emission expected in the TRACE 171 Å band according to model B. After the first 5 minutes, the loop gets brighter and brighter gradually and everywhere at the same rate. The brightness is much higher at the footpoints at any time, and the contrast footpoints/apex ranges between more than two orders of magnitude ($t \approx 300$ s) and ~ 30 at the end of the simulation. Although the data suggest us to reject *a priori* any totally symmetric heating, the uniform heating model B predicts that the region around the loop apex brightens later than the footpoints, as it is observed. It is also interesting to note that the temperature maximum is coincident with the density minimum at the loop apex, due to pressure balance; this leads to a very low brightness of the apex, because of the low emission measure and of the temperature outside the instrument sensitivity band, and therefore to the high contrast between the brightness at the footpoints and at the apex. This high contrast is against the observation and suggests us that the heating rate must be either lower or non-constant, to have the plasma at a lower temperature for a relatively long time.

We work in the hypothesis of a symmetric initial atmosphere. One may wonder if a symmetric heating in a strongly asymmetric initial atmosphere may yield the observed asymmetric evolution. We think this is unlikely, mainly because a symmetric heating would invariably lead to simultaneous (although not identical) bright fronts from the footpoints, the same reason why we can reject the non-thermal beam heating hypothesis (see Sect. 5). We remark also that, if present, strong initial asymmetries may have some importance only at the dense footpoints; as shown above, elsewhere the initial atmosphere is very thin and cool, and the details of the temperature and density distributions are unimportant, because the plasma evolution is dominated by the dense, fast and hot plasma fronts coming up from the chromosphere.

4.1.3. Asymmetric heating

The data and the models illustrated above show us that the heating cannot be entirely symmetric and uniform, nor it can be concentrated at the footpoints, nor at the apex. In addition, the case of heating at the footpoint suggests us that the heating is likely to be located in the southern leg, i.e. in the side of the loop opposite to that of the brighter and earlier brightness fronts. Indeed, the relative timing of the brightness fronts arising from the two footpoints suggests us that a plausible location of the heating is intermediate between the apex and the southern footpoint, and, in particular, at $\sim 1/3$ of the loop length. In model C, the heating is switched on at a distance 3×10^9 cm from the left footpoint (which is the southern one in the observation) and kept constant for 3000 s (case C in Table 4.1). The heating extent along the loop is assumed $\sigma = 5 \times 10^8$ cm[5].

As shown in Fig. 7, the temperature and density evolutions and their timing are in some way similar to those of the case of uniform heating (model B) described in Sec.4.1.2, but the fundamental difference is that they are clearly asymmetric with respect to the loop apex. Indeed, the evolution is much more complex than it appears at first glance. In fact, the conduction front propagates from the center of the heated region, and arrives first at the left footpoint ($t \sim 100$ s) and slightly later at the other footpoint. Since then, the temperature distribution grows higher but its shape no longer changes significantly, remaining slightly asymmetric with a smooth maximum at the center of the heating distribution. The earliest density front arises (at $t \sim 160$ s, i.e. about one minute later) from the left footpoint, with a speed reaching ~ 130 km/s. The evaporative front originating from the other footpoint moves slightly later and slower, with a speed below 60 km/s. However accumulation of plasma on the right side makes the latter front denser than the former one. At the same time the temperature on the right side is lower than on the heated side. Both these effects determine a more luminous front in the TRACE 171 Å band on the *right side* of the loop, the *non-heated* one. Eventually ($t > 1000$ s) the plasma slows down, and the plasma fills up the loop more gradually and uniformly. Near the end of the simulation the temperature maximum (≈ 1.5 MK) is still at the center of the heating distribution, where the density has a corresponding minimum ($\approx 2 \times 10^8$ cm^{-3}), because of pressure balance.

In the TRACE 171 Å filter band, at first only the footpoints are visible, while faint brightness fronts move from them. A bright front rises from the right footpoint at $t \approx 500$ s, and reaches the loop apex at $t \approx 1000$ s. Then the brightness increases gradually everywhere along the loop. The brightness distribution along the loop is steadily asymmetric after the propagation of the initial bright fronts: the right leg and footpoint are the brighter ones. In other words, at the heating position we find, once again, a brightness *minimum* in the TRACE band, because there the temperature is maximum and the density is minimum: both these effects contribute to decrease the emission in the rather narrow band of TRACE, as discussed in Section 4.1.2. We have checked that moderate modifications of the intensity (a factor 2) and spatial extent σ (a factor 2) of the heating, do not induce significantly different results.

The evolution predicted by this model resembles the observed evolution much more closely than the other two discussed before. In particular two features are well reproduced: i) the sequence of moving brightness fronts and their relative timing; ii) the asymmetric shape of the brightness distributions along the loop during all the rising phase. None of the other cases described before is able to match both constraints. We come to the conclusion that *the heating which determines the loop brightening is very likely released between the southern footpoint and the apex.*

On the other hand, there are still some details which do not match the observation, and, in particular: a) the brightness contrasts footpoints/apex predicted by the model of asymmetric heating is high, significantly higher than the observed one at any time; b) the brightness is significantly lower than the observed one, almost anywhere along the loop.

The footpoints/apex contrasts may be reduced by reducing the total heating rate injected in the loop; this would in fact reduce the temperature in the central loop regions and make it fall more within the TRACE sensitivity range, thus increasing the apparent brightness at the apex, while slightly reducing it at the footpoints. We have verified, however, that a smaller amount of heating would lead to a much more

[5]Of the same order of the size of structure **B**.

gradual evolution and to much less plasma evaporation. The loop plasma would therefore emit even less, making problem b) even worse.

4.2. Variable heating

In order to get a better match to the data the heating should, on the one hand, lead to the same general characteristics of the evolution and brightness distribution as obtained in case C of Table 4.1, but, at the same time, to denser and cooler plasma for most of the time. One way to meet these requirements is to assume still an asymmetric heating at the same location as in model C (to match the time sequence of the observed moving fronts), but not constant after turn on. The heating should be initially intense, in order to obtain a strong conduction front and a strong plasma evaporation, but should then decay rapidly, in order to let the plasma cool down and become well visible in the TRACE sensitivity range. The temperature of the loop would be high in the initial phases of the evolution, while the loop is still empty. With an appropriate timing of the heating decay, the evaporating plasma, however, would travel along the loop while both the heating and the temperature are decreasing, therefore obtaining a plasma at the same time dense and relatively cool, as observed. Such an impulsive and then decaying heating is expected also on the basis of theoretical considerations (Litwin and Rosner 1993).

The point is to tune up the right combination of timing and intensity parameters of the heating needed to reproduce both the observed timing of the evolution and the detailed brightness levels and contrasts. Since the task is indeed a difficult one, we will not attempt to match perfectly all the observational data, but a general matching of all of the above requirements will be enough for us.

4.2.1. Abrupt switch off

Our first attempt has been to study what happens to the loop if the heating is switched off abruptly. By switching it off at t = 2000 s, we notice that the brightness distribution then changes radically and, in particular, the contrast footpoints/apex *decreases* rapidly and becomes less than 10 at the peak of luminosity. Although the predicted overall loop luminosity is indeed too low with respect to the observed one, this simulation shows that a decaying heating is in the right direction to explain the observed low contrast footpoints/apex.

4.2.2. Constant high plus exponentially decaying heating

It is difficult to fine tune the temporal parameters of the transient heating, since the brightness increases while the heating decreases, and there is no direct tracer of the heating evolution. We have, therefore, proceeded further by trial and error. In the following we present the results for a model of heating which is suddenly switched on, stays high (ten times that in model C) and constant for 100 s, and then it decays exponentially with an e-folding time of 300 s. We will call this model **C'** (see Table 4.1).

As shown in Fig. 8, the high intensity of the heating makes the local temperature increase rapidly to a maximum of $\sim$ 3 MK; in less than 20 sec it becomes more than 1 MK in $\sim$ 90% of the loop, due to the high efficiency of thermal conduction and the low initial plasma density. The earliest evaporation front develops from the left footpoint, the closest to the heating location, with a velocity up to 250 km/s. The density front from the other footpoint is slower ($\sim$ 150 km/s) but steeper. They meet at a distance $\sim 4 \times 10^9$ cm from the right footpoint at $t \approx 300$ s, causing a local density excess. Then the density increases more gradually, with a smooth front propagating leftwards and reaching the left footpoint at $t \approx 1200$ s. The pressure settles uniformly between 0.1 and 0.2 dyne cm^{-2} at $t \approx 300$ s but it decreases gradually for $t > 1000$ s. At t = 3000 s the pressure is everywhere below 0.1 dyne cm^{-2} and highest at the right footpoint.

Given the high initial temperature, the early and most dynamic plasma evolution is practically invisible to TRACE in the 171 Å band: only the footpoints become bright and the left one is temporarily brighter than the other one. The footpoints/apex contrast begins to decrease significantly only after 10 minutes since the beginning of the heating. This occurs because the heating is decreasing, the coronal plasma is cooling and entering more and more into the TRACE sensitivity range. Therefore TRACE would begin to see the rest of the loop brighten after more than 10 minutes from the beginning of the heating, and it would first detect a brightness front propagating from the *right* footpoint, as apparent from the asymmetric shape of the brightness distribution at that time. A brightness front rises from the other footpoint with a delay of $\sim$ 5 minutes. Then the loop brightens more gradually and uniformly, while the footpoints get gradually fainter. The brightness contrast footpoints/apex decreases below a factor 10 after about half an hour since the beginning of the heating. Then the entire loop slowly begins to fade away. The footpoints fade asymmetrically, first ($t \approx 2200$ sec) the right one.

The loop evolution[6] as it would be detected by TRACE is also illustrated in Fig.9, to be compared to that of Fig.2. Note that the first significant brightness front rises from the right footpoint after 10 minutes since the initial brightening of the footpoints, and a less intense one from the left footpoint after other ~ 6 minutes. The chronological order and the relative timing of the brightness fronts are in reasonable agreement with the observed evolution: even the delay of ~ 400 s of the left front is matched (see Section 2 in this paper and Section 3.3 in Paper I). In the assumption that the heating function and parameters are approximately correct, by matching the times at which the model and observed brightness fronts from the right footpoints begin to propagate, i.e. $t \approx 600$ s and $t \approx 2500$ s (see Section 2), respectively, we trace back the start time of the heating at $t \approx 1900$ s from the beginning of the observation, i.e. just at the time when the loop footpoints become well visible, immediately after a data gap. This appears as a self-consistent result. Note that the model predicts the right footpoint to decay first and this is consistent to the observed decay of the northern footpoint, after the rising phase (see Paper I).

5. Discussion

As shown in Section 4 we have been able to reproduce many of the observed features of the brightening of loop L_4 and to put strong constraints on the modeling. This has been made possible by some conditions:

- The high quality of the data: the above results could not have been obtained with a lower spatial resolution or a less frequent image sampling rate;
- A particularly well observed loop structure: although included in a region crowded by other structures, L_4 is well isolated from the other bright structures, it has a very well defined geometry (i.e. shape and size) which changes little during the time lapse that we model, i.e. the rising phase. The evolution is monitored since the beginning of the brightening, and the loop evolves coherently as a single filament during the rising phase.

The relatively simple and constant geometry of the loop structure, and its coherent evolution, allow us to model this event with a purely hydrodynamic approach and with a one-dimensional description. The great advantage is the small number of free parameters of the modeling, once data analysis has constrained the dimensions and the range of physical conditions of the plasma to be studied. Such a "tuned" modeling, combined with the high quality of the data, offers a unique opportunity to constrain well the physical parameters, and in particular the heating parameters.

Once excluded that the loop becomes visible just because it is cooling from a hotter state into the TRACE temperature sensitivity range, we have been able to discriminate among possible locations of the heating which ignites the loop and to exclude a uniform, or even just symmetric, heating and a heating concentrated at one of the footpoints. We did not include the possibility of a heating located at both footpoints and asymmetric, such as that by twin electron beams impinging on asymmetric footpoints. Although we cannot rule out this possibility on the basis of detailed computations, we do not plan to do them in the future, because there are too many unconstrained parameters, as further discussed below. One issue, in our opinion, makes heating by non-thermal electron beams inadequate to drive the observed loop evolution: the beams of (relativistic) electrons would hit against the footpoints practically simultaneously, and they would produce two simultaneous evaporation fronts, although not necessarily symmetric. The observation tells us instead that there is a distinct and measurable delay between the brightness fronts arising from the footpoints. One may think of beams triggered at one time in one direction and, later, only in the opposite direction but this would be hardly reasonable. Analogously we have not considered heating deposited directly at both footpoints: one should have a good reason for two far-away sites of the heating which would turn on at different times and would have to be "ad hoc" correlated to yield the observed

[6] An animation of the sequence is available at http://www.astropa.unipa.it/....

evolution. There would be a much higher number of free parameters and no compelling physical reason for the two heating sites. Since we can explain observations with just one heating site, Occam's razor argument leads us to prefer model C'.

Our analysis and modeling has allowed us to obtain the following constraints on:

Geometry : a vertical model loop cannot reproduce the observed evolution while an inclined loop does it much better, thus confirming the indications coming from purely geometric and morphological arguments;

Initial conditions : once excluded that we observe a cooling loop, the fact that the loop is initially invisible and the simulations tell us that the loop plasma must be initially cool ($\lesssim 10^5$K) and it cannot be initially very dense, nor too tenuous, but in a limited range of density values, namely those described in section 3.2.

Heating location : most of the heating is likely deposited in the southern leg, at a position intermediate between the footpoint and the apex ($\sim 3 \times 10^9$ cm since the southern footpoint).

Heating timing : the observed brightness profiles and timing are best reproduced with a heating which starts after about half an hour from the beginning of the observation, is high for a couple of minutes and then decays rapidly with a characteristic time scale of a few minutes.

We remark that we have not aimed at a detailed fitting of the observational data and at reproducing *exactly all* the observed features. Nevertheless the accurate comparison with the data and the extensive exploration of alternative models provide significant and constraining indications and allow us to derive a clear and self-consistent scenario: a magnetic loop inclined on the surface, initially empty, and subject to a highly transient heating episode in the southern leg of the loop. Further refinements of the modeling would have led to no significant progress in our insight into the loop evolution and may have introduced too many free parameters.

The modeling is a valuable tool to gain insight into the physical evolution of the loop plasma. It shows us that the observed evolution is produced by a combination of plasma dynamics and of its thermal evolution. In particular, the heating first produces an invisible conduction front which heats the loop and, as it reaches the footpoints, makes the dense chromospheric plasma expand upwards into the corona. Because of the asymmetric position of the heating, the loop legs brighten not simultaneously, and the loop brightness distribution remains asymmetric at all times.

According to model C', the heating brings the loop very rapidly to a high temperature, above that of TRACE peak sensitivity. The initial very dynamic phase with the fast propagation of plasma fronts is not detectable in the TRACE band because it is very faint. Instead TRACE detects the combination of slower plasma upflows and of plasma cooling into the TRACE temperature sensitivity range, which occurs during the heating decay. The footpoints cool earlier and the upper loop regions progressively follow, giving the impression of a moving front. This "thermal" front sums up with the proper relatively slow plasma upflow ($\sim$ 50 km/s) and determines the observed apparently higher brightness propagation speed of $\sim$ 100 km/s.

Although plasma evaporation may not be the only and direct cause of the detected brightness fronts, it is however a necessary component in our modeling to determine the observed evolution: the loop needs to be initially empty, otherwise regions other than the footpoints would invariably brighten first, as shown in Section 3.2.

We have inferred the position of the heating from the relative timing of the observed brightness fronts, with the aid of the insight provided by preliminary simulations. This position is the one which best reproduces both the profiles of the brightness and its time-evolution. Therefore the heating location appears to be tightly constrained. It is interesting to note that at the heating position the modeling predicts a *minimum* of the emission detected by TRACE, because both the temperature is a maximum, outside the maximum TRACE sensitivity range, and the density, and therefore also the emission measure, is a minimum. Of course, this is in part a consequence of the TRACE narrow spectral band, but a low emission measure can really be a general feature of the heating location.

Also the total heating rate is rather well constrained: less heating would not produce enough evaporation, more would make the loop too hot. We have simply assumed the heating extent along the loop (σ) to be of the order of the size of structure **B**, which seems to have a role in the loop evolution, as further discussed below. Strong constraints on σ can hardly come from the modeling because of the high efficiency of thermal conduction along the magnetic field lines. We just notice that the heating distribution cannot be much wider than the assumed one, otherwise the evolution would become similar to that of the rejected case of uniform heating (model B).

Although our modeling cannot say much about the heating distribution *across* the magnetic field lines, the fact that during the rising phase the loop evolves coherently as a single filament indicates that the heating width across the loop is likely to be of the same order as the loop diameter itself (see Paper I). This is not a new indication: Litwin & Rosner (1993) bring solid theoretical arguments to show that such large transverse size of the heating is tied to heating time scales of the order of the loop turn-on time. Longer time scales would lead to a more localized heating. One may then speculate as follows: our modeling predicts that later on, after the initial impulsive phase, the heating decays on longer time scales; according to the above considerations, it is then expected to act on smaller parts of the loop section. This is indeed in agreement to what is observed: after the luminosity maximum, several individual loop filaments appear to evolve, and therefore to be heated independently of each other.

Finally, as for the time evolution of the heating, our "best" model C' implies a heating initially high and then exponentially decaying. Only such a time-structured heating can account for the observed relatively low footpoint/apex contrast. The heating rate is ten times the one required to maintain the loop steadily at $T \sim 1$ MK. Such an impulsive behavior, and even the factor 10, have been suggested on the basis of theoretical considerations by Litwin and Rosner (1993). The present study not only confirms this indication, but provides quantitative figures for the rate and characteristic time scales of the heating matching a specific case. Model C' is able to reproduce quite well the relative timing of the brightness fronts and this has led us to estimate $t \sim$ 13:32 UT as a possible start time of the heating. This time is just after a major data gap and is the time at which the loop footpoints brighten. We do not exclude that different possible choices of the time evolution of the heating may lead to place the heating start at earlier (unlikely later) times.

From the parameters of model C' we can make quantitative estimates on the global energetics and on the magnetic fields involved in the event. The total heating injected in the model loop is $E_H \approx 6 \times 10^{26}$ erg with a peak rate of 1.5×10^{24} erg/s, by assuming a cross sectional area $\approx 3 \times 10^{17}$ cm^2. The heating volume is $V \approx 4 \times 10^{26}$ cm^3. The magnetic field cancelled to produce the heating can be estimated as $\Delta B \sim 8\pi E_H/(2\ B\ V) \sim 18/B \sim 0.2 - 2$ G, for an unperturbed magnetic field $B \sim 10 - 100$ G. For a plasma at pressure $p_{max} \simeq 0.1$ dyne/cm^2 to be confined in a rigid loop, a minimum magnetic field $B_{min} \simeq \sqrt{8\pi p_{max}} \simeq 2$ G is required. These values are fully consistent, and represent a moderate perturbation, to the values of $\sim 100 - 200$ G of the photospheric magnetic field at the loop footpoints, derived from the magnetogram (see Paper I). On the other hand, since the cross-section is fairly constant along the loop, one may argue that the magnetic field intensity in the loop may not be much lower than the photospheric values. All this produces a reasonably self-consistent scenario.

As a final remark, it is instructive, at this point, to look back carefully at the observation in the light of what we have learnt from the modeling. If we focus our attention on the position of the heating suggested by the modeling, we realize that a structure is visible there for the whole duration of the heating: the structure that we named **B** in Paper I, and which appears as a bundle of short and variably bright filaments (see also Section 2). It is then natural to wonder whether this structure is physically connected to the heating deposition or not, or even coaligned by chance. We note that, as mentioned in Paper I, the linear size of structure B is approximately 15", i.e. $\sim 10^9$ cm, comparable to the loop cross section diameter. This length is also of the same order as the height of the heating location above the solar surface, thus suggesting that the structure may extend from the solar surface to the loop L_4 with a compact shape. Therefore, although one cannot exclude other hypotheses, the loop may be interacting with structure B, e.g. be the site of magnetic reconnective processes, and not be aligned along the same line of sight by chance. The loop brightening may also be connected to the highly dynamic event observed in the same region before the beginning of the brightening. Structure B may then be a tracer of the heating deposition in the soft X-rays.

6. Conclusions

We have analyzed the ignition of a coronal loop monitored by TRACE. The high quality of the observation has allowed us to tune up a detailed hydrodynamic modeling of the plasma confined in the loop leaving few free parameters, and to have a tight feedback on the choice of the parameters from the comparison of the synthesized emission to the observed one. This has led us to gain physical insight into the plasma evolution and to put significant constraints on the loop transient heating. Although the loop has been modelled as an isolated system, our analysis has suggested us some possible physical connections to surrounding structures and to their (dynamic) evolution.

Although the episode described here of course cannot be exhaustive of the scenarios for loop coronal heating, the location of the loop heating is well constrained, together with its temporal evolution. It indicates a heating localized *in corona* and impulsive, which may help to discriminate among the proposed heating mechanisms (e.g. Narain and Ulmshneider 1996).

A systematic search for the structures analogous to the one we suggest as tracer of the heating, i.e. structure **B**, may provide important information on the coronal heating. The high spatial resolution of instruments like TRACE may allow an important insight into the filamentation or, more in general, the morphology of such structures.

FR, GP and SS acknowledge support from Ministero della Ricerca Scientifica e Tecnologica and Agenzia Spaziale Italiana. EED and LG were supported by Contract No. NAS5-38099 from NASA to LMATC. We thank Ms. R.A. McMullen for assistance with the data analysis and with mission operations.

REFERENCES

Antiochos, S.K., 1984, ApJ, 280, 416.

Betta, R., 1998, Ph.D. Thesis.

Betta, R. M., Peres, G., Serio, S., Reale, F., 1997, A&AS 122, 585.

Cargill, P.J., Priest, E.R., 1980, Sol. Phys., 65, 251.

Doscheck, G.A., Cheng, C.C., Oran, E.S., Boris, J.P., Mariska, J.T., 1983, ApJ, 265, 1103.

Feldman, U., 1992, Physica Scripta, 46, 202.

Fisher, G.H., Canfield R.C., McClymont, A.N., 1985, ApJ, 289, 414.

Gan, W. Q., Zhang, H. Q., Fang, C., A&A, 241, 618.

Hori, K., Yokoyama, T., Kosugi, T., Shibata, K., 1997, ApJ, 489, 426.

Kopp, R. A., Poletto, G., 1993, ApJ, 418, 496.

Litwin, C., & Rosner, R., 1993, ApJ, 412, 375.

Mariska, J.T., Boris, J.P., 1983, ApJ, 267, 409.

MacNeice, P., 1986, Sol. Phys., 103, 47

Mewe, R., Kaastra, J. S., Liedhal, D. A. 1995, Legacy 6, 16

Narain, U., Ulmschneider P., 1996, Space Science Rev., 75, 453.

Nagai, F., 1980, Sol. Phys., 68, 351

Nagai, F., Emslie, A.G., 1984, ApJ, 279, 896

Noci, G., 1981, Sol. Phys., 69, 63.

Orlando, S., Peres, G., Serio, S., 1995, A&A, 294, 861.

Peres, G., Reale, F., Serio, S., Pallavicini, R., 1987, ApJ, 312, 895.

Peres, G., Reale, F., Serio, S., 1993, in Physics of Solar and Stellar Coronae, J. L. Linsky and S. Serio eds., Kluwer Academic Publ., p. 151.

Peres, G., Rosner, R., Serio, S., Vaiana, G. S., 1982, ApJ 252, 791.

Raymond, J. C., Smith, B. W., 1977, ApJS 35, 419.

Reale, F., Peres, G., 1995, A&A, 299, 225

Reale, F., Peres, G., 1999, ApJL, submitted.

Reale, F., Peres, G., Serio, S., DeLuca, E.E., Golub, L., 1999, ApJ, submitted (Paper I).

Rosner, R., Tucker, W., Vaiana, G., 1978, ApJ, 220, 643.

Serio, S., Peres, G., Vaiana, G.S., Golub, L., Rosner, R., 1981, ApJ, 243, 288.

Vaiana, G.S., Krieger, A.S., Timothy, A.F., 1973, Sol. Phys., 32, 81.

Vernazza, J. E., Avrett, E. H., Loeser, R., 1980, ApJS 45, 619.

Vesecky, J. F., Antiochos, S. K., Underwood, J. H., 1979, ApJ, 233, 978.

Fig. 1.— Sketch (in scale) of Loop L_4 and of the main other structures surrounding it. Three other loops and the irregular filamentary structure B are present.

Fig. 2.— Brightness distribution along loop L_4 measured by TRACE in the 171 Å band at various times (in seconds since the beginning of the observation). For a detailed comparison with the results of modeling the brightness has been background subtracted and averaged in sectors along the loop as discussed in Paper I. The values obtained have then been mapped onto a one-dimensional loop-like semicircular structure for ease of comparison with model computations. The left footpoint in the pictures corresponds to the southern loop footpoint. The grey scale is in DN/s/pix.

Fig. 3.— Model loop geometry (upper sketch) including orientation with respect to the vertical. We show the location and width of the loop transient heating (dark bands) for the models in Table 1. The different grey tones indicate the relative intensity of the heating.

Fig. 4.— Evolution of the plasma temperature, density, pressure, velocity and emission per unit volume in the TRACE 171 Å band along the model loop heated at the left footpoint (Model A in Table 1). Each distribution is sampled at the labeled time (in seconds since the beginning of the heating). In the velocity plot, curves after 500 sec are dashed (to avoid confusion with the other curves). In the lower left panel, the observed brightness distributions (*diamonds*) at t=1875 s (lower) and at t=3374 s (upper) are also shown assuming a conversion factor from flux to model emission of 10^{-9} cm^{-1}.

Fig. 5.— The grey scale loop-shaped pictures show emission distributions in the TRACE 171 Å band as the last panel of Fig.4, at the labeled times (in seconds since the beginning of the model heating), for comparison to the data shown in Fig.2. The grey scale is in units of 10^{-9} DN cm^{-1} s^{-1} pix^{-1}.

Fig. 6.— As Fig.4 for the model loop heated uniformly (Model B in Table 1). The assumed conversion factor of the data to model emission is 0.5×10^{-9} cm^{-1}.

Fig. 7.— As Fig.4 for the model loop heated asymmetrically on the right leg (Model C in Table 1). The

assumed conversion factor of the data to model emission is 0.5×10^{-9} cm^{-1}.

Fig. 8.— As Fig.4 for model loop C': the heating is on the right leg (as model C in Table 1) but constant high for 100 s and then exponentially decaying with an e-folding time 300 s. The pressure at t = 3000 s is dashed for the sake of clarity. The assumed conversion factor of the data to model emission is 0.5×10^{-9} cm^{-1}.

Fig. 9.— As Fig.5 for the loop model C'.

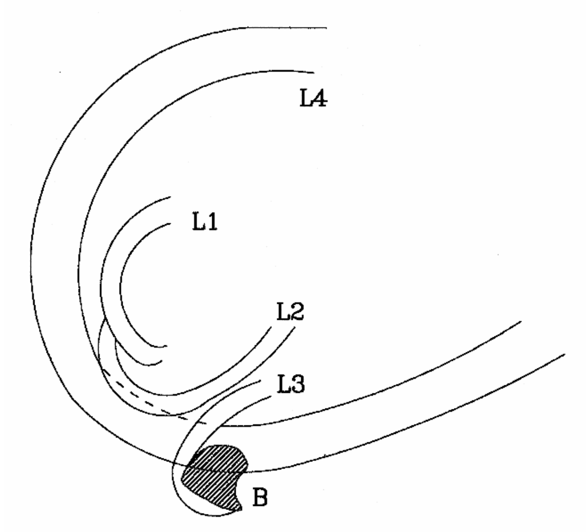

Fig. 1.—

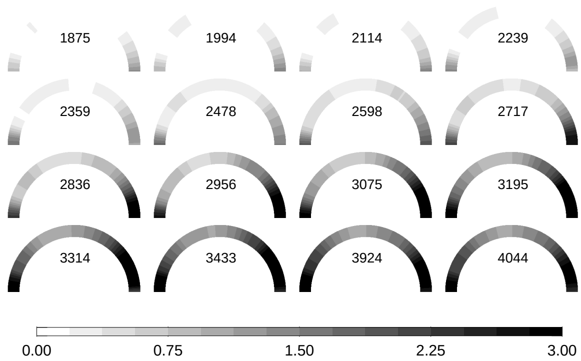

Fig. 2.—

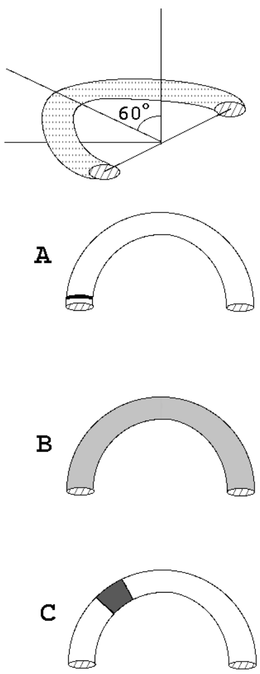

60°
A
B
C

Fig. 3.—

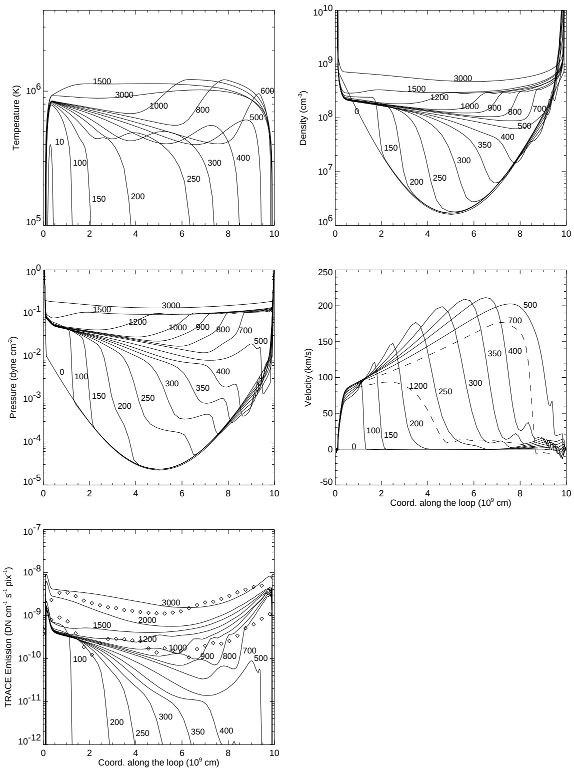

Temperature (K)
Density (cm^{-3})
Pressure (dyne cm^{-2})
Velocity (km/s)
TRACE Emission (DN cm^{-1} s^{-1} pix^{-1})
Coord. along the loop (10^9 cm)

Fig. 4.—

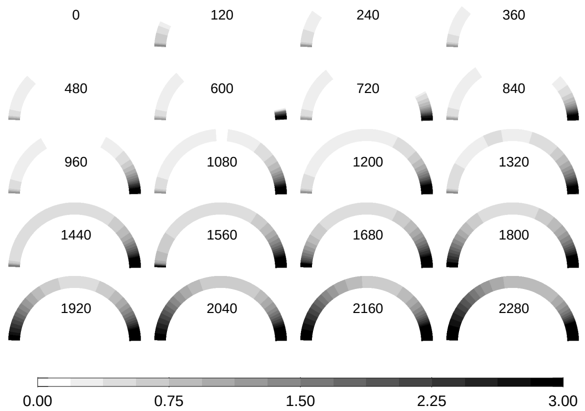
0
120
240
360
480
600
720
840
960
1080
1200
1320
1440
1560
1680
1800
1920
2040
2160
2280
0.00
0.75
1.50
2.25
3.00

Fig. 5.—

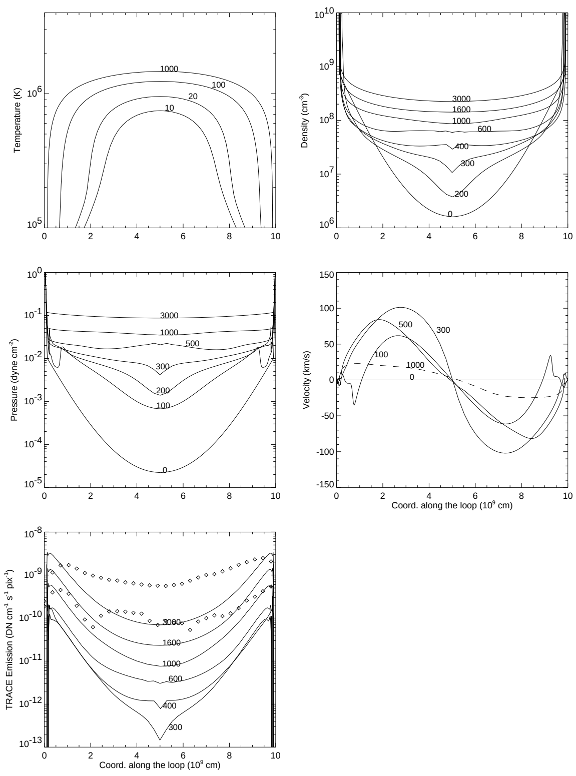
Temperature (K)
Density (cm-3)
Pressure (dyne cm-2)
Velocity (km/s)
TRACE Emission (DN cm-1 s-1 pix-1)
Coord. along the loop (10^9 cm)

Fig. 6.—

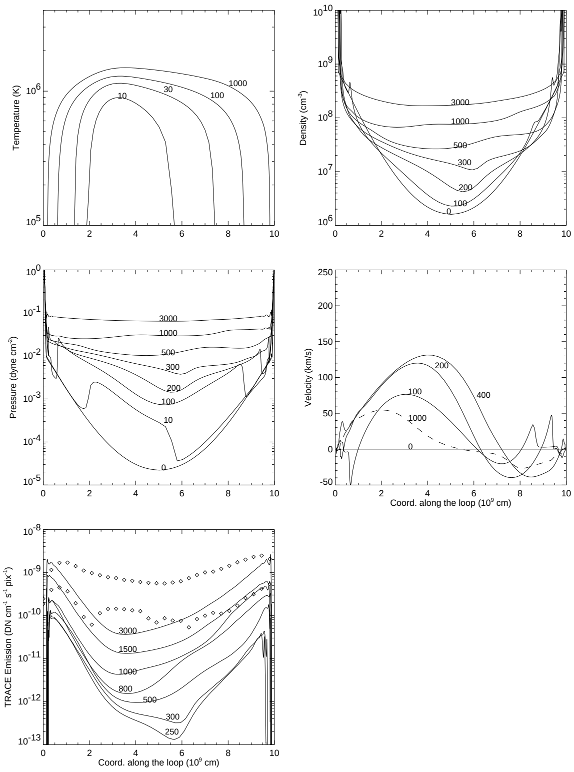
Temperature (K)
Density (cm-3)
Pressure (dyne cm-2)
Velocity (km/s)
TRACE Emission (DN cm-1 s-1 pix-1)
Coord. along the loop (10^9 cm)

Fig. 7.—

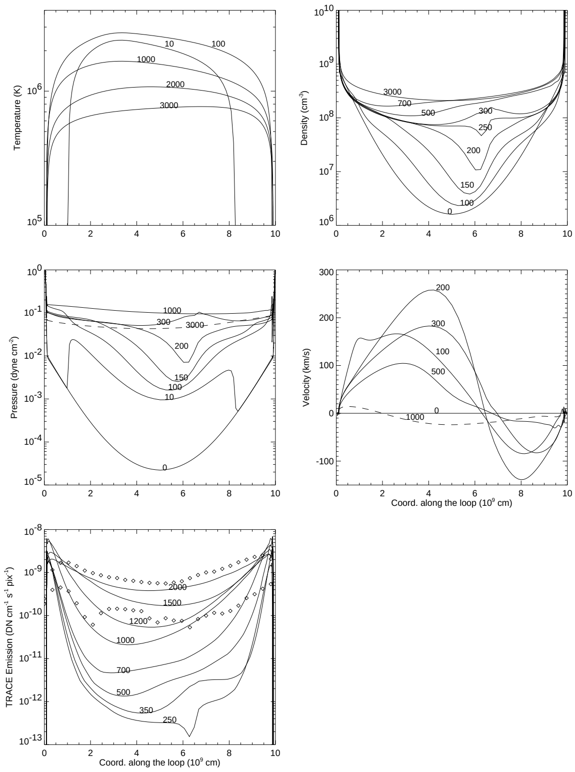
Temperature (K)
Density (cm-3)
Pressure (dyne cm-2)
Velocity (km/s)
TRACE Emission (DN cm-1 s-1 pix-1)
Coord. along the loop (10^9 cm)

Fig. 8.—

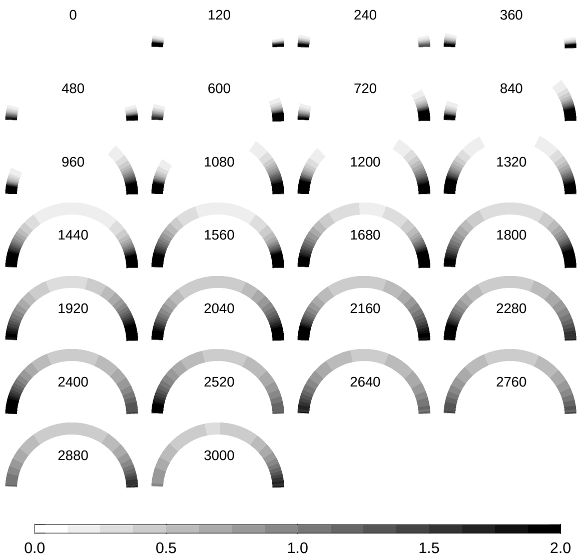
0
120
240
360
480
600
720
840
960
1080
1200
1320
1440
1560
1680
1800
1920
2040
2160
2280
2400
2520
2640
2760
2880
3000
0.0
0.5
1.0
1.5
2.0

Fig. 9.—